Journal of Chemical Crystallography (2025) 55:281–289
https://doi.org/10.1007/s10870-025-01059-0

ORIGINAL PAPER

Synthesis, Crystal Structure, FT-IR and UV-Vis Spectra of Tetranuclear Copper (II) Complex with 4-methoxypyridine as Co-Ligand

Ugur Erkarslan[1] · Gorkem Oylumluoglu[1] · Ozay Eroglu[2] · Hanife Sevval Dere[2] · Elif Gungor[3] · Hulya Kara Subasat[2] · Adem Donmez[4]

Received: 26 May 2025 / Accepted: 1 August 2025 / Published online: 21 August 2025

Abstract

A methanol solvate of the tetranuclear Cu(II) complex with 4-methoxypyridine (4-MOP) as co-ligand have been synthesized, $[Cu_4OCl_6.(4\text{-MOP})_4].CH_2OH$, (4-MOP=4-methoxypyridine) and characterized by IR, UV–Vis spectroscopy and single crystal X-ray diffraction. The complex exhibits a tetrahedral $\{Cu_4O\}$ core, where four Cu(II) ions are bridged by six chloride ligands and further stabilized through coordination with 4-methoxypyridine ligands. Each copper center displays a distorted trigonal bipyramidal geometry. Intermolecular C–H···Cl and C–H···O hydrogen bonds interconnect the molecules, forming a three-dimensional supramolecular framework. Spectroscopic data, including UV-Vis and FT-IR, substantiate the formation of the Cu_4O cluster and align with the structural observations. These findings offer valuable insights into the coordination behavior and supramolecular organization of μ_4-oxo copper complexes, presenting a useful model for biomimetic systems and a potential foundation for applications in catalysis and material science.

Graphical Abstract

A rare example of a μ_4-oxo-bridged tetranuclear Cu(II) complex stabilized by 4-methoxypyridine ligands has been selectively synthesized and structurally characterized. This is among the few known Cu_4OCl_6 type architectures incorporating 4-MOP, revealing a well-defined $\{Cu_4O\}$ core and a 3D supramolecular network through weak hydrogen bonding.

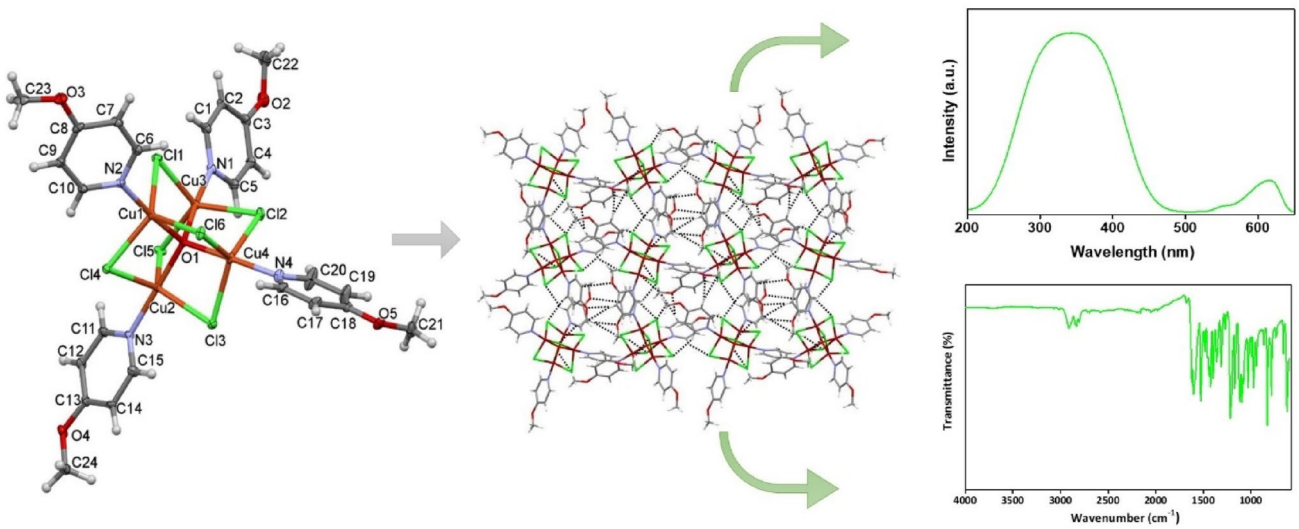

Keywords Cu(II) complex · Crystal structure · 4-methoxypyridine · Spectroscopy

Extended author information available on the last page of the article

Introduction

The synthesis and characterization of oxygen-bridged metal complexes have attracted considerable interest due to their potential as structural and functional models in bioinorganic chemistry [1, 2]. This interest arises because many enzymes and proteins, particularly those involved in redox-active processes, incorporate metal centers in their active sites [3, 4]. For instance, ferritin is a key iron-storage protein complex that regulates the human body's solubilization, storage, and release of dietary iron [5, 6]. Similarly, in cyanobacteria and plants, manganese oxidation is essential for the water-splitting reaction in photosystem II [7].

Copper-containing enzymes such as laccase [8], tyrosinase [9], ascorbate oxidase [10], catechol oxidase, cytochrome C oxidase [11], and methane monooxygenase [12] exemplify the crucial roles of copper centers in biological oxidation reactions. Furthermore, copper complexes, particularly those involving polynuclear cores, are widely used as catalysts due to their ability to mediate multi-electron transfer reactions in coordination with ligand systems [13, 14].

Although various copper complexes have been synthesized and explored for catalytic and biological relevance, there remains a gap in the systematic study of μ4-oxo-bridged tetranuclear copper clusters featuring biologically compatible ligands. Such complexes are relatively rare in the literature and hold significant potential as models for multicopper oxidases and other metalloenzymes due to their structural resemblance and electron-transfer capabilities [15, 16]. In particular, the use of methoxy-substituted pyridyl ligands offers a new direction for tuning the electronic and steric environment around the copper centers, potentially affecting the redox behavior and stability of the complexes [17, 18].

Despite its potential, the use of 4-methoxypyridine (4-MOP) as a co-ligand in transition metal coordination chemistry has been relatively limited. This is primarily attributed to the methoxy oxygen's low propensity for coordination, restricting 4-MOP to act predominantly as a terminal ligand through its pyridine nitrogen donor [19]. Nevertheless, structurally characterized 4-MOP complexes have been reported with 5d metals such as Pt, Hf, Re, Ir, and W, as well as with 4d metals including Ru, Pd, and Ag. Additionally, examples involving Cd(II), Fe(II), Zn(II), Co(III), Ni(II), and Cu(II) have been documented, highlighting the versatile yet underexplored coordination chemistry of this ligand type [20, 21]. These studies suggest that 4-MOP may offer valuable electronic and steric modulation, particularly in polynuclear architectures, but its role remains insufficiently investigated within oxo-bridged copper systems [22].

Herein, we present the synthesis, crystal structure and spectroscopic properties of a unique μ4-oxo-bridged tetranuclear copper complex $[Cu_4OCl_6.(4\text{-MOP})_4]$ (4-MOP = 4-methoxypyridine). This complex may serve as a valuable model for biological redox systems, offering new insights into the design of polynuclear copper assemblies incorporating 4-MOP ligands.

2. Materials and Methods

2.1. Materials and Measurements

All chemical reagents and solvents were purchased from Sigma-Aldrich and used as received without further purification. The solid-state UV-Vis spectrum was recorded using an Ocean Optics Maya 2000-PRO spectrometer, while the IR spectrum was obtained using a PerkinElmer Spectrum 65 FT-IR spectrometer. Single-crystal X-ray diffraction measurements were carried out at 273 K using a three-circle CCD diffractometer with graphite-monochromated Mo-K_α radiation ($\lambda = 0.71073$ Å). The SAINT software package integrated the intensity data [23]. Absorption, Lorentz, and polarization corrections were applied. The structures were solved by direct methods and refined by full-matrix least-squares against $|F|^2$ using the OLEX2 software suite [24]. All non-hydrogen atoms were refined with anisotropic displacement parameters without positional restraints. Hydrogen atoms were positioned in idealized geometries and included in the refinement using isotropic displacement parameters constrained to 1.2 times the equivalent isotropic displacement (U_{equiv}) of their parent carbon atoms. Hydrogen bonding interactions were analyzed using PLATON v1.17 [25], and molecular visualizations were performed using MERCURY [26].

The methanol molecules in the crystal lattice appear to be highly disordered, and it was difficult to reliably model their positions and distribution. Therefore, the MASK function of the OLEX2 program was used to eliminate the contribution of the electron density in the solvent region from the intensity data, and the solvent free model was employed for the final refinement. The disordered methanol molecules were not included in the molecular weight given in Table 1, and their atoms are also excluded from the atomic list in Table 2.

2.2. Synthesis of $[Cu_4OCl_6(4\text{-MOP})_4]$ Methanol Solvate

We employed a slow diffusion method known as the "mini H-tube" technique to obtain single crystals suitable for X-ray analysis. This technique was chosen for its ability

Table 1 Crystallographic data for the complex

CCDC No	2,277,253
Molecular weight	$C_{24}H_{28}C_6Cu_4N_4O_5$ [+CH_3OH]
Molecular weight (g mol^{-1})	919.36
Crystal system	Monoclinic
Space group	C2/c
Unit cell parameters	a = 18.271(4) α = 90
	b = 18.242(4) β = 99.85(3)
	c = 21.157(4) γ = 90
V ($Å^3$)	6948(3)
Z	8
T (K)	100(2)
h index	−23 ≤ h ≤ 23, −23 ≤ k ≤ 23, -27 ≤ l ≤ 27
ρ_{calc} (g/cm^3)	1.758
μ (mm^{-1})	2.916
F(000)	3664
Crystal size	0.2 × 0.2 × 0.1 mm^3
2Θ range for data collection	3.178 to 54.968
Refinement method	Full-matrix least-squares on $\|F\|^2$
Reflections collected	34,486
Independent reflections	7969 [R_{int}=0.049]
Observed reflections > 2σ(*I*)	6589 F
Final R indexes [I >= 2σ (I)]	R_1 = 0.0383, wR_2 = 0.0776
Final R indexes [all data]	R_1 = 0.0501, wR_2 = 0.0820
Data/restraints/parameters	7969/0/392
S	1.02
Largest diff. peak and hole (e $Å^{-3}$)	0.73 and −0.52

to produce high-quality single crystals suitable for X-ray analysis, which is crucial for the structural characterization of the complex. This approach allowed stoichiometric amounts of 4-methoxypyridine and $CuCl_2$ to diffuse slowly toward each other under controlled conditions.

Initially, 4-methoxypyridine (0.2 mmol) was dissolved in 5 mL of deionized water, while $CuCl_2$ (0.2 mmol) was dissolved in 10 mL of a 1:1 (v/v) mixture of deionized water and methanol. Each solution was transferred into separate small glass tubes. These inner tubes were placed inside a larger sealed glass vessel (with a cap), which was filled with deionized water to allow for slow and controlled diffusion.

After the diffusion process was completed, green single crystals formed within the inner tubes. The crystals were collected by vacuum filtration, washed sequentially with deionized water, methanol, and diethyl ether, and dried at room temperature.

As the process yielded single crystals suitable for X-ray diffraction through slow diffusion without bulk product isolation, it is more accurately described as a crystallization rather than a conventional synthesis. Therefore, no isolated reaction yield is reported.

Table 2 Selected dond lengths and bond angles (Å, °)

Bond lengths			
Cl1-Cu3	2.3788 (10)	Cl6-Cu4	2.4187 (12)
Cl1-Cu1	2.3856 (9)	Cl6-Cu1	2.4367 (10)
Cl2-Cu4	2.3739 (10)	Cu1-O1	1.905 (2)
Cl2-Cu3	2.3807(11)	Cl5-Cu2	2.4344 (9)
Cl3-Cu2	2.3977 (10)	Cu2-O1	1.907 (2)
Cl3-Cu4	2.4039 (9)	Cu3-O1	1.916 (2)
Cl4-Cu1	2.3978 (9)	Cl5-Cu3	2.4122 (9)
Cl4-Cu2	2.4052 (11)	Cu4-O1	1.909 (2)
Bond angles			
O1-Cu1-N2	174.88 (10)	O1-Cu3-N1	175.61 (10)
O1-Cu1-Cl1	85.56 (7)	O1-Cu3-Cl1	85.50 (7)
N2-Cu1-Cl1	90.41 (8)	N1-Cu3-Cl1	98.36 (8)
O1-Cu1-Cl4	85.11 (7)	O1-Cu3-Cl2	84.74 (7)
N2-Cu1-Cl4	99.73 (8)	N1-Cu3-Cl2	91.57 (8)
Cl1-Cu1-Cl4	122.15 (3)	Cl1-Cu3-Cl2	118.03 (3)
O1-Cu1-Cl6	84.25 (7)	O1-Cu3-Cl5	84.73 (7)
N2-Cu1-Cl6	95.29 (8)	N1-Cu3-Cl5	95.49 (8)
Cl1-Cu1-Cl6	122.45 (3)	Cl1-Cu3-Cl5	114.80 (4)
Cl4-Cu1-Cl6	113.12 (3)	Cl2-Cu3-Cl5	124.89 (4)
O1-Cu2-N3	178.77 (10)	O1-Cu4-N4	178.03 (10)
O1-Cu2-Cl3	84.16 (7)	O1-Cu4-Cl2	85.07 (7)
N3-Cu2-Cl3	96.14 (8)	N4-Cu4-Cl2	94.46 (9)
O1-Cu2-Cl4	84.85 (7)	O1-Cu4-Cl3	83.93 (6)
N3-Cu2-Cl4	93.97 (8)	N4-Cu4-Cl3	94.62 (9)
Cl3-Cu2-Cl4	120.71 (4)	Cl2-Cu4-Cl3	117.92 (4)
O1-Cu2-Cl5	84.31 (7)	O1-Cu4-Cl6	84.66 (7)
N3-Cu2-Cl5	96.55 (8)	N4-Cu4-Cl6	97.20 (8)
Cl3-Cu2-Cl5	120.39 (4)	Cl2-Cu4-Cl6	121.88 (4)
Cl4-Cu2-Cl5	116.11 (4)	Cl3-Cu4-Cl6	117.54 (3)

The elemental analysis of the obtained complex $[C_{24}H_{28}Cl_6Cu_4N_4O_5].CH_3OH$, calculated C 31.56, H 3.39, N 5.89%; Found: C 31.54, H 3.37, N 5.86%.

3. Results

3.1. Crystal Structure

The complex crystallizes in the monoclinic crystal system with space group C2/c. The asymmetric unit consists of one molecule of $[Cu_4OCl_6(4\text{-MOP})_4]$, and also contains disordered methanol. As depicted in Fig. 1, the fundamental structure of the complex is based on a tetrahedral μ4-oxo-centered $\{Cu_4O\}$ core, where six halide Cl^- ions each bridge a pair of copper(II) ions. Four 4-methoxy pyridine ligands are coordinated to the copper centers via nitrogen atoms, forming a well-defined tetranuclear unit. Moreover, similar Cu···Cu distances and Cu–O–Cu angular parameters have been reported in structurally analogous $\{Cu_4OCl_6\}$ clusters [27–29], supporting the consistency of this tetranuclear arrangement.

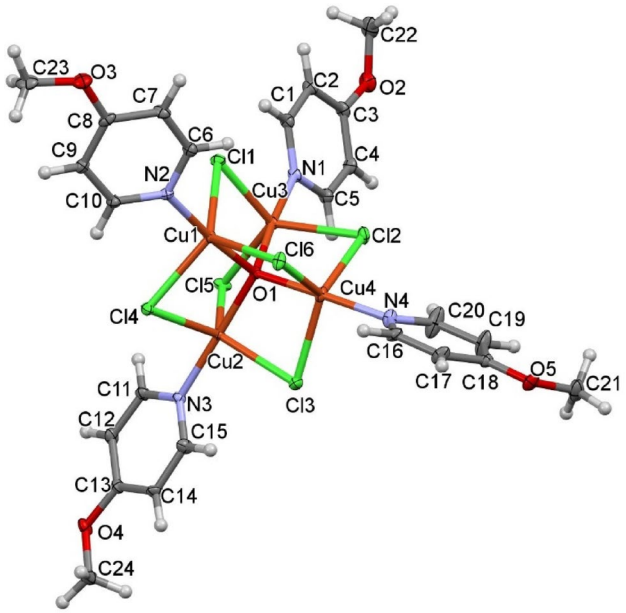

Fig. 1 The molecular structure of the complex

The coordination geometry around each copper atom can be described as a distorted trigonal bipyramid, defined by one nitrogen atom from 4-MOP, the central oxo-bridge oxygen atom, and three bridging chloride ligands. The Cu–N bond lengths fall within the range of 1.965(3)–1.978(3) Å, while Cu–O distances are 1.905(2)–1.916(2) Å, and Cu–Cl distances vary between 2.374(11)–2.437(11) Å. The intramolecular Cu···Cu distances range from 3.092 to 3.134 Å, which are in agreement with previously reported [$Cu_4OCl_6L_4$] complexes [15–17, 28, 30, 31]. Comparable Cu···Cu distances and coordination geometries have also been documented by Behrens et al. [32], who showed that such clusters exhibit high structural stability and possible catalytic behavior in redox processes.

The complex exhibits significant intermolecular hydrogen bonding interactions. As shown in Fig. 2, C–H···Cl hydrogen bonds between neighboring {Cu_4OCl_6} units result in the formation of one-dimensional chains, which further organize into a two-dimensional supramolecular network through C–H···O interactions. These two-dimensional layers stack along the b-axis to form a three-dimensional packing motif (Fig. 3).

Both C–H···Cl and C–H···O are classified as weak hydrogen bonds, yet they play a crucial role in the organization and stabilization of the crystal structure. The importance of such interactions in crystal engineering has been extensively documented. For instance, Aakeröy et al. [33] emphasized the structural significance of C–H···Cl interactions, while Derewenda et al. [34] highlighted the role of C–H···O bonds in forming 2D networks and stabilizing supramolecular architectures. Additionally, Langfelderová et al. [35] demonstrated that weak hydrogen bonds significantly influence the thermal behavior of Cu(II) complexes, linking structure with decomposition pathways. Table 1 summarizes crystallographic data, and Table 2 lists selected bond lengths and angles. Hydrogen bonding parameters are detailed in Table 3.

3.2. Spectroscopic Properties

The solid-state UV-Vis spectrum of the complex was recorded in the wavelength range of 250–700 nm (Fig. 4). The peak observed at 335 nm can be attributed to a combination of π→π* and n→π* transitions within the aromatic ring of the 4-methoxypyridine ligand. A weak absorption band at 615 nm in the visible region corresponds to the d–d transitions of the Cu(II) ion, which is consistent with typical copper(II) complex behavior [36].

FT-IR spectroscopy was employed to confirm the coordination behavior of 4-methoxypyridine (4-MOP) with the Cu(II) center and to investigate structural differences between the free ligand and its complex (Fig. 5). In the high wavenumber region, the aliphatic C–H stretching bands of 4-MOP, originally observed at 2933 cm^{-1} and 2841 cm^{-1}, shift slightly to 2921 cm^{-1} and 2847 cm^{-1} in the complex. Such red shifts are commonly associated with subtle changes in the electron density distribution caused by coordination, and have similarly been reported for Cu(II) complexes with alkyl-substituted pyridines [37]. One of the most significant changes upon coordination is observed in the C=N and C=C stretching regions, where free 4-MOP exhibits a prominent band at 1522 cm^{-1}, assigned to pyridine ring vibrations. This band shifts to 1507 cm^{-1} in the complex, while the 1430 cm^{-1} band remains nearly constant at 1431 cm^{-1}. These changes are consistent with coordination through the pyridine nitrogen atom and are in excellent agreement with both experimental and theoretical studies of Cu(II)-pyridine type ligands [37, 38]. As Wong and Brewer emphasized, even small shifts in the ν(C=N) stretching region can be strong indicators of coordination via the nitrogen atom in Cu(II)–pyridine systems [38]. In the 1300–1000 cm^{-1} region, subtle but meaningful shifts are also present. The C–O stretching vibration of the methoxy group, found at 1130 cm^{-1} in free 4-MOP, appears at 1120 cm^{-1} in the complex. While this oxygen is not directly involved in coordination, the shift may arise due to conjugative interactions between the methoxy substituent and the coordinated pyridine ring [37, 41]. Additional ring vibrations at 1343 and 1217 cm^{-1} in 4-MOP shift to 1324 and 1215 cm^{-1} in the complex, suggesting perturbations in the electronic environment of the aromatic system upon metal binding, a trend similarly observed in Cu(II) and Mn(II) complexes with methoxypyridine derivatives [39, 40]. In

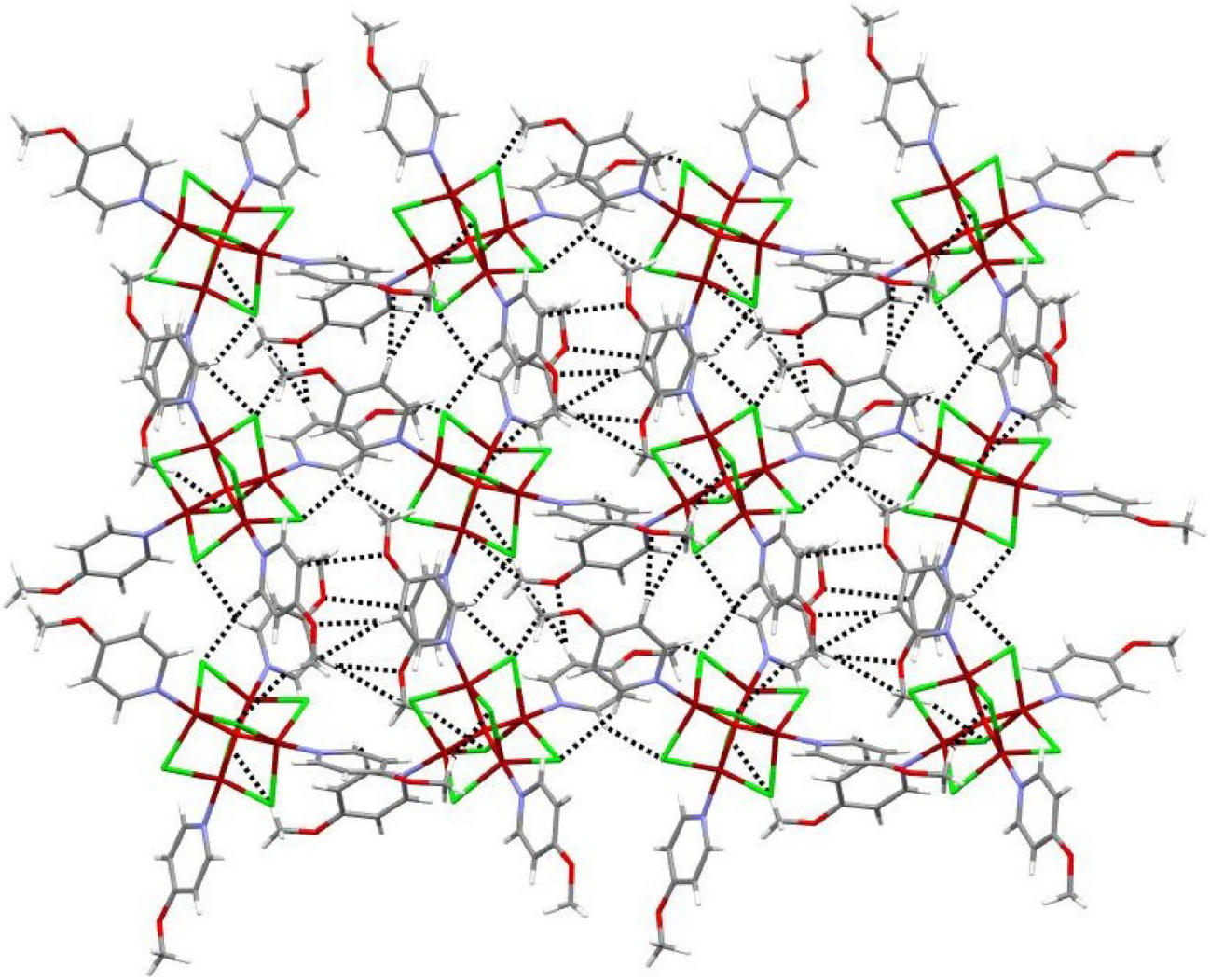

Fig. 2 Two-dimensional network formed via hydrogen bonding interactions

the fingerprint region, bands at 930 cm^{-1} and 727 cm^{-1} in the complex are shifted from 950 cm^{-1} and 713 cm^{-1} in the ligand, corresponding to ring deformation and out-of-plane bending vibrations, respectively. These types of shifts are commonly reported in pseudohalide [41] and pyridine-based Cu(II) coordination compounds [37], and support a coordination-induced geometric rearrangement. Notably, in line with previous findings, no distinct bands attributable to Cu–N stretching were observed in the 400–600 cm^{-1} region, likely due to instrumental cutoff or overlapping absorptions [38, 41]. Overall, the observed spectral shifts—particularly in the ν(C=N), ν(C–H), and ν(C–O) regions—strongly support the coordination of 4-MOP to the Cu(II) center through its pyridine nitrogen. These findings are consistent with previous reports on related copper(II) complexes with methoxypyridine and pseudohalide ligands, confirming the reliability of FT-IR as a diagnostic tool for identifying coordination sites [37, 38–41].

4. Conclusions and Discussion

In this study, a novel μ_4-oxo-bridged tetranuclear copper(II) complex, $[Cu_4OCl_6(4\text{-MOP})_4].CH_2OH$, incorporating 4-methoxypyridine (4-MOP) as a co-ligand, was successfully synthesized and structurally characterized through single-crystal X-ray diffraction, FT-IR, and UV–Vis spectroscopy. The structural analysis revealed that the complex adopts a $\{Cu_4O\}$ tetrahedral core in which four copper centers are interconnected via six chloride bridges and coordinated to 4-methoxypyridine ligands through nitrogen atoms. Each copper ion exhibits a distorted trigonal bipyramidal coordination environment.

The crystal packing is stabilized by a network of weak C–H···Cl and C–H···O hydrogen bonds, resulting in a two-dimensional supramolecular network that extends into a three-dimensional framework. These hydrogen bonding interactions play a critical role in the stability and

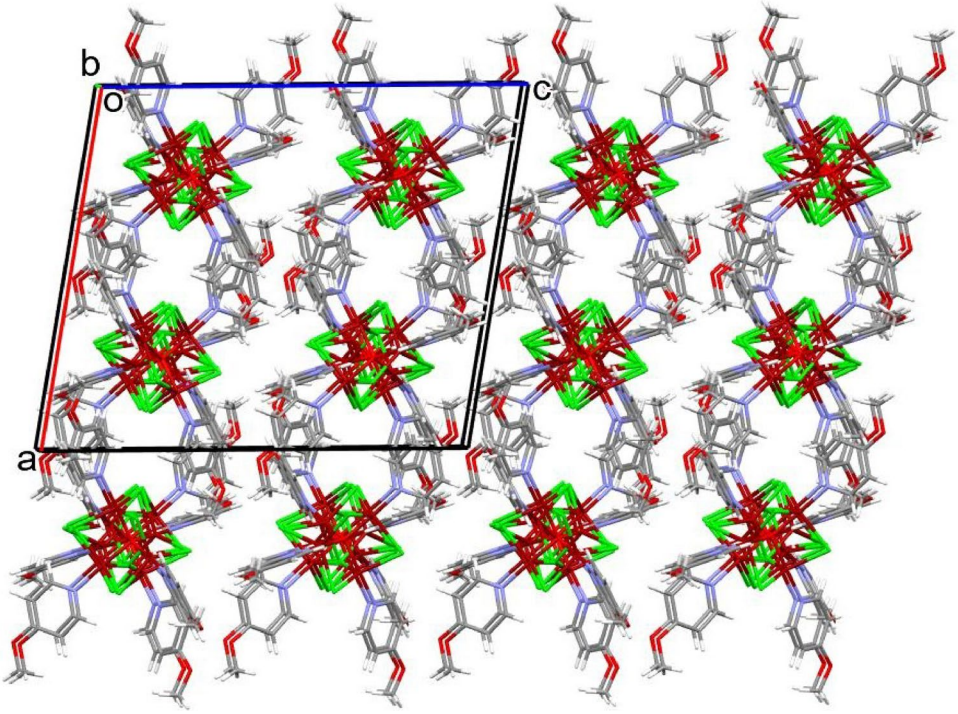

Fig. 3 The three-dimensional packing structure of the complex is viewed along the a-axis

Table 3 Hydrogen bonds (Å, °)

D–H···A*	D–H	H···A	D···A	D–H···A	Symmetry
C1–H1···Cl1	0.95	2.69	3.332(19)	125	
C4–H4···O4	0.95	2.58	3.453(20)	153	1/2+x, −1/2+y, z
C7–H7···O5	0.95	2.55	3.419(20)	153	−1/2+x, −/2+y, z
C10–H10···Cl4	0.95	2.76	3.396(19)	125	
C10–H10···Cl4	0.95	2.77	3.609(21)	148	−x, y, 1/2−z
C11–H11···Cl5	0.95	2.78	3.360(19)	120	
C15–H15···Cl3	0.95	2.69	3.290(18)	122	
C16–H16···Cl6	0.95	2.77	3.369(19)	122	
C20–H20···Cl2	0.95	2.63	3.223(18)	121	
C21–H21C···Cl5	0.98	2.74	3.644(21)	154	1−x, y, 1/2−z
C24–H24A···Cl6	0.98	2.78	3.656(21)	149	x, −y, −1/2+z

organization of the crystal structure, demonstrating the importance of weak interactions in crystal engineering.

Spectroscopic studies further corroborated the structural findings. The UV-Vis spectrum displayed characteristic absorption bands corresponding to ligand-centered π→π* and n→π* transitions as well as d–d transitions associated with the copper(II) centers. The FT-IR spectrum confirmed the coordination of the 4-MOP ligands to the copper ions through shifts in characteristic vibrational bands.

The successful isolation and characterization of this complex contribute to a deeper understanding of the coordination behavior of 4-methoxypyridine with copper(II) centers, which remains underexplored. Moreover, the structural features of the $\{Cu_4O\}$ core offer valuable insights for the design of new polynuclear copper-based systems with potential applications in catalysis and biomimetic chemistry. Future work could explore the catalytic properties of such μ_4-oxo tetranuclear complexes and their behavior under redox-active conditions, providing a bridge between structural models and functional applications in bioinspired systems.

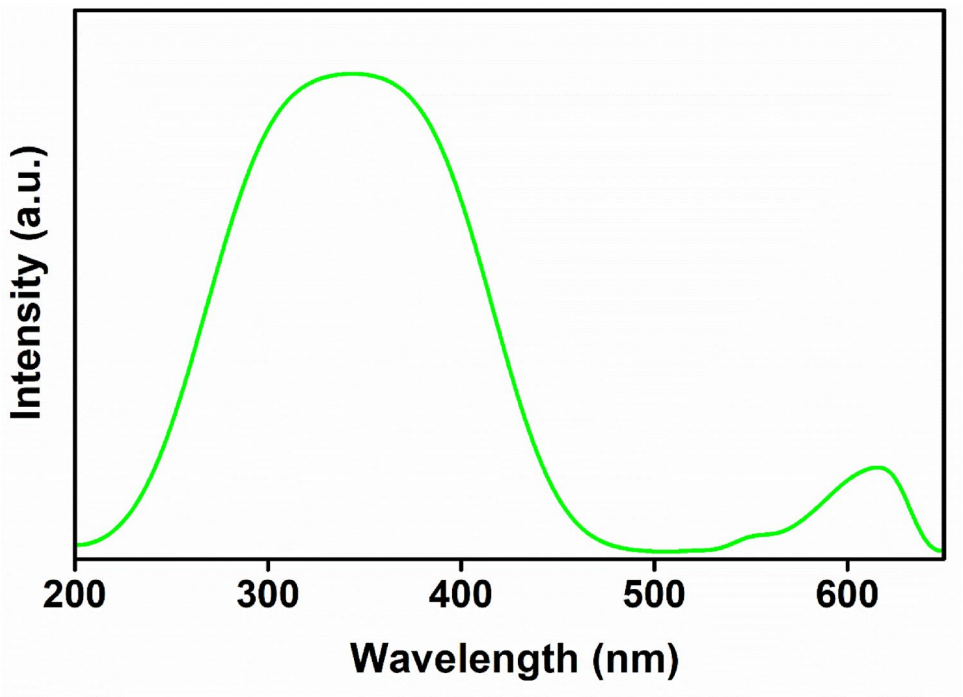

Fig. 4 Solid-state UV-Vis spectrum of the complex

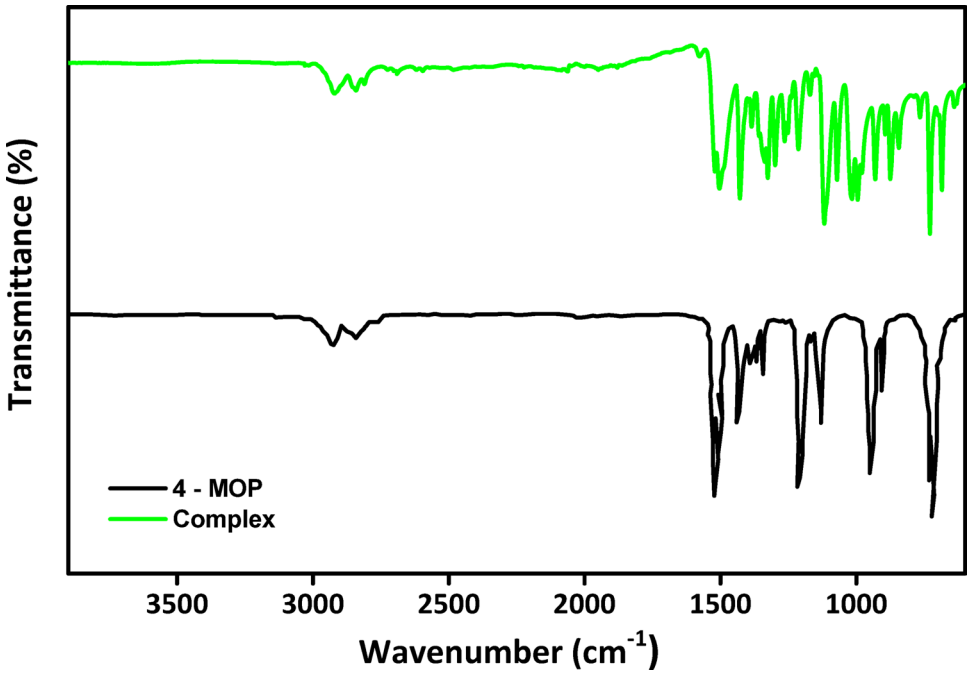

Fig. 5 Solid-state FT-IR spectra of the Cu(II) complex and the free 4-methoxypyridine (4-MOP) ligand

Supplementary Information The online version contains supplementary material available at https://doi.org/10.1007/s10870-025-01059-0.

Author Contributions U.E. Conceptualization, Experimental Design, Writing – Original DraftG.O. Conceptualization, Experimental Design, Writing – Original DraftO.E. Investigation, Experiments, Visualization, ResourcesH.S.D. Investigation, Experiments, Visualization, ResourcesE.G. Investigation, Experiments, Visualization, ResourcesH.K.S. Investigation, Visualization, Writing – Original Draft PreparationA.D. Investigation, Visualization, Writing – Original Draft Preparation.

Funding This research did not receive any specific grant from funding agencies in the public, commercial, or not-for-profit sectors.

Data Availability All data generated or analyzed during this study are included in this published article. The crystallographic data for the complex discussed in the article have been deposited at the Cambridge Crystallographic Data Centre (CCDC). They are available free of charge upon request using the deposition number CCDC 2277253. Requests for data can be made via: Address: The Director, CCDC, 12 Union Road, Cambridge CB2 1EZ, United Kingdom Email: deposit@ccdc.cam.ac.uk Website: http://www.ccdc.cam.ac.uk Fax: +44 1223 336033.

Declarations

Conflict of interest The authors declare that there is no conflict of interest regarding the content of this article.

Ethical Approval The authors declare that they have complied with all ethical standards during this study.

References

1. Arar W, Ali RB, El May MV, Khatyr A, Jourdain I, Knorr M, Brieger L, Scheel R, Strohmann C, Chaker A, Akacha AB (2023) Synthesis, crystal structures, and biological activities of halogen-(oalkylphenylcarbamothioate) bis (triarylphosphine) copper(I) complexes. J Mol Struct 1284:135370. https://doi.org/10.1016/j.molstruc.2023.135370
2. Massoud SS, Louka FR, Salem NMH, Fischer RC, Torvisco A, Mautner FA, Vančo J, Belza J, Dvořák Z, Trávníček Z (2023) Dinuclear doubly bridged phenoxide copper(II) complexes as efficient anticancer agents. Eur J Med Chem 246:114992
3. De Boer JW, Browne WR, Feringa BL, Hage R (2007) Carboxylate-bridged dinuclear manganese systems – from catalases to oxidation catalysis. C R Chim 10:341–354. https://doi.org/10.1016/j.crci.2006.09.018
4. Hai Y, Dugery RJ, Healy D, Christianson DW (2013) Formiminoglutamase from *Trypanosoma cruzi* is an arginase-like manganese metalloenzyme. Biochemistry 52:9294–9309. https://doi.org/10.1021/bi401352h
5. Bou Abdallah F, Papaefthymiou GC, Scheswohl DM, Stanga SD, Arosio P, Chasteen ND (2002) μ-1,2-peroxo-bridged di-iron(III) dimer formation in human h-chain ferritin. Biochem J 364:57–63. https://doi.org/10.1042/bj3640057
6. Kongchoo S, Chainok K, Kantacha A, Wongnawa S (2017) Nickel-based hexaazamacrocyclic complexes: structure, spectroscopy and catalytic properties. Inorg Chem Commun 83:97–102. https://doi.org/10.1016/j.inoche.2017.06.024
7. Zhou MH, Lin JY, Zhang WP, Jian JX, Wondu Dagnaw F, Wang T, Tong QX (2023) Solar-driven water splitting using copper terpyridine complexes as OER catalysts. Solar RRL 7:2201018. https://doi.org/10.1002/solr.202201018
8. Bonomo RP, Castronovo BMG, Santoro AM (2004) A spectroscopic investigation of the interaction between the fungal laccase's nitrogen monoxide and copper sites from Rigidoporus diagnosis. Dalton Trans 1:104–112. https://doi.org/10.1039/B313630B
9. Matoba Y, Kumagai T, Yamamoto A, Yoshitsu H, Sugiyama M (2006) Crystallographic evidence of flexibility in the dinuclear copper center of tyrosinase during catalysis. J Biol Chem 281:8981–8990. https://doi.org/10.1074/jbc.M509785200
10. Gromov I, Marchesin A, Farver O, Pecht I, Goldfarb D (1999) Azide binding to the trinuclear copper center in laccase and ascorbate oxidase. Eur J Biochem 266:820–830. https://doi.org/10.1046/j.1432-1327.1999.00898.x
11. Carr HS, Winge DR (2003) Assembly of cytochrome c oxidase within the mitochondrion. Acc Chem Res 36:309–316. https://doi.org/10.1021/ar0200807
12. Lieberman RL, Rosenzweig AC (2005) Crystal structure of a membrane-bound metalloenzyme that catalyzes biological oxidation of methane. Nature 434:177–182. https://doi.org/10.1038/nature03311
13. Becker S, Dürr M, Miska A, Becker J, Gawlig C, Behrens U, Ivanović-Burmazović I, Schindler S (2016) Copper chloride catalysis: do μ4-oxide copper clusters play a significant role? Inorg Chem 55:3759–3766. https://doi.org/10.1021/acs.inorgchem.5b02576
14. Zhou MH, Lin JY, Zhang WP, Jian JX, Wondu Dagnaw F, Wang T, Tong QX (2023) Solar-driven water splitting in photovoltaic electrolysis systems using copper terpyridine complexes as oxygen evolution catalysts. Solar RRL 7:2201018–2220101. https://doi.org/10.1002/solr.202201018
15. Jammi S, Punniyamurthy T (2009) Synthesis, structure, and catalysis of tetranuclear copper(II) open cubane for Henry reaction on water. Eur J Inorg Chem 2009:2508–2511. https://doi.org/10.1002/ejic.200900141
16. Löw S, Becker J, Würtele C, Miska A, Kleeberg C, Behrens U, Walter O, Schindler S (2013) Reactions of copper(II) chloride in solution: formation of tetranuclear copper clusters. Chemistry – A European Journal 19:5342–5351. https://doi.org/10.1002/chem.201203848
17. Gungor E, Kara H, Colacio E, Mota AJ (2014) Two tetranuclear copper(II) complexes with open cubane-like Cu_4O_4 core framework and ferromagnetic exchange interactions: structure, magnetic properties, and DFT study. Eur J Inorg Chem 2014:1552–1560. https://doi.org/10.1002/ejic.201301515
18. Kocak C, Oylumluoglu G, Donmez A, Coban MB, Erkarslan U, Aygun M, Kara H (2017) Crystal structure and photoluminescence properties of a new monomeric copper(II) complex. Acta Crystallographica Section C: Structural Chemistry 73(5):414–419. https://doi.org/10.1107/S2053229617005976
19. Uçar İ, Vural H, Küçük E (2015) Two chelidamate complexes with 4-methoxypyridine: a theoretical and experimental study. Spectrochim Acta A Mol Biomol Spectrosc 151:667–672. https://doi.org/10.1016/j.saa.2015.07.023
20. Mautner FA, Traber M, Fischer RC, Reichmann K, Vicente R (2018) Pseudohalide-metal(II) complexes with 4-methoxypyridine co-ligand: synthesis and characterization. Polyhedron 144:30–35. https://doi.org/10.1016/j.poly.2018.01.012
21. Tamer Ö (2017) A manganese(II) complex of 4-methoxypyridine-2-carboxylate: synthesis, crystal structure, FT-IR, UV–Vis and DFT. J Mol Struct 1144:370–378. https://doi.org/10.1016/j.molstruc.2017.05.077
22. Perry JJ, McManus GJ, Zaworotko MJ (2004) 4-methoxypyridine-(pyridine-2,6-dicarboxylato-N,O, O′)copper(II). J Chem Crystallogr 34(12):877–882
23. Bruker (1998) SMART and SAINT. Bruker AXS, Madison, WI, USA
24. Dolomanov OV, Bourhis LJ, Gildea RJ, Howard JAK, Puschmann H (2009) OLEX2: a complete structure solution, refinement and analysis program. J Appl Crystallogr 42:339–341. https://doi.org/10.1107/S0021889808042726
25. Spek AL (2009) Structure validation in chemical crystallography. Acta Crystallogr Sect D Biol Crystallogr 65(2):148–155. https://doi.org/10.1107/S090744490804362X
26. Macrae CF, Edgington PR, McCabe P, Pidcock E, Shields GP, Taylor R, Towler M, van de Streek J (2006) Mercury: visualization and analysis of crystal structures. J Appl Crystallogr 39:453–457. https://doi.org/10.1107/S002188980600731X
27. Churchill MR, Rotella FJ (1979) Stereochemistry of four-coordinate copper(II). Inorg Chem 18(6):1666–1670
28. Cortés P, Atria AM, Garland MT, Baggio R (2006) Three oxo complexes with a tetranuclear $[Cu_4(\mu_2\text{-}Cl)_6(\mu_4\text{-}O)]$ unit. Acta Crystallographica Section C: Structural Chemistry 62:m311–m314. https://doi.org/10.1107/S0108270106021354
29. Bertrand JA, Kelley BE (1966) The crystal structure of tetrakis(μ-chloro)tetra-μ-oxotetracopper(II). Inorg Chem 5(1):16–20
30. Liu YY, Grzywa M, Weil M, Volkmer D (2010) $[Cu_4OCl_6(DABCO)_2]\cdot 0.5DABCO\cdot 4CH_3OH$: a zeolite-like MOF from Cu_4OCl_6 SBUs. J Solid State Chem 183:208–217. https://doi.org/10.1016/j.jssc.2009.10.026

31. Valenzuela J, Atria AM, Spodine E et al (1999) Magnetostructural study of μ4-oxo Cu4 complexes. Inorg Chem 38(25):5681–5685
32. Behrens U, Kleeberg C et al (2016) Structural and catalytic properties of oxo-bridged Cu(II) clusters. Inorg Chim Acta 453:69–75
33. Aakeröy CB, Evans TA, Seddon KR, Pálinkó I (1999) The C-H··· Cl hydrogen bond: does it exist? New J Chem 23(2):145–152. https://doi.org/10.1039/A809309A
34. Derewenda ZS, Lee L, Derewenda U (1995) The occurrence of C-H··· O hydrogen bonds in proteins. J Mol Biol 252(2):248–262. https://doi.org/10.1006/jmbi.1995.0492
35. Langfelderová H, Máková D, Jorík V (1994) Thermolysis of hydrated Cu(II) complexes. Thermochim Acta 243:145–151
36. Gliemann GABP (1985) ABP Lever: Inorganic Electronic Spectroscopy, Vol. 33, Studies in Physical and Theoretical Chemistry. Elsevier, Amsterdam. https://doi.org/10.1002/bbpc.19850890122
37. Malik M, Świtlicka A, Bieńko A, Komarnicka UK, Bieńko DC, Kozieł S et al (2022) Copper(II) complexes with 2-ethylpyridine and hydroxyl pyridine derivatives: structural, spectroscopic, magnetic and anticancer studies. RSC Adv 12(42):27648–27665. https://doi.org/10.1039/D2RA04996F
38. Wong PT, Brewer DG (1968) The coordination bond in copper complexes of substituted pyridines: far-IR spectra and force constants. Can J Chem 46(2):139–148. https://doi.org/10.1139/v68-025
39. Mautner FA, Fischer RC, Zoroddu MA, Strehblow HH, Reiss GJ (2018) A unique manganese(II) complex of 4-methoxypyridine-2-carboxylic acid: structural and spectroscopic characterization. Polyhedron 144:30–35. https://doi.org/10.1016/j.poly.2018.01.012
40. Fodor L, Mihaly J, Szabo T, Pusztai L, Marek T (2017) Two new chelidamate complexes with the 4-methoxypyridine: synthesis, structure, and FT-IR studies. J Mol Struct 1149:329–336
41. Gölcü A, Tümer M, Demirelli H, Wheatley RA (2005) Synthesis and characterization of pseudohalide–metal(II) complexes and their spectroscopic properties. Spectrochim Acta A 61(11–12):2311–2317. https://doi.org/10.1016/j.saa.2004.09.003

Authors and Affiliations

Ugur Erkarslan[1] · Gorkem Oylumluoglu[1] · Ozay Eroglu[2] · Hanife Sevval Dere[2] · Elif Gungor[3] · Hulya Kara Subasat[2] · Adem Donmez[4]

✉ Gorkem Oylumluoglu
gorkem@mu.edu.tr

[1] Department of Physics, Faculty of Science, Molecular Nano-Materials Laboratory, Mugla Sitki Kocman University, Mugla, Turkey

[2] Department of Energy, Molecular Nano-Materials Laboratory, Mugla Sıtkı Kocman University, Muğla, Turkey

[3] Department of Physics, Faculty of Arts and Sciences, Balikesir University, Balikesir, Turkey

[4] Department of Electricity and Energy, Yatagan Vocational School, Mugla Sitki Kocman University, Mugla, Turkey